Article

Studies of Ancient Russian Cultural Objects Using the Neutron Tomography Method

Sergey Kichanov [1,*]**, Irina Saprykina** [2]**, Denis Kozlenko** [1]**, Kuanysh Nazarov** [1]**, Evgenii Lukin** [1]**, Anton Rutkauskas** [1] **and Boris Savenko** [1]

[1]   Frank Laboratory of Neutron Physics, Joint Institute for Nuclear Research, 141980 Dubna, Russia; denk@nf.jinr.ru (D.K.); quanysh@list.ru (K.N.); lukin@jinr.ru (E.L.); ranton@nf.jinr.ru (A.R.); savenko@nf.jinr.ru (B.S.)

[2]   Institute of Archaeology Russian Academy of Sciences, 117036 Moscow, Russia; dolmen200@mail.ru

*   Correspondence: ekich@nf.jinr.ru; Tel.: +7-496-216-2112

Abstract: Neutron radiography and tomography is a non-destructive method that provides detailed information about the internal structure of cultural heritage objects. The differences in the neutron attenuation coefficients of constituent elements of the studied objects, as well as the application of modern mathematical algorithms to carry out three-dimensional imaging data analysis, allow one to obtain unique information about the spatial distribution of different phases, the presence of internal defects, or the degree of structural degradation inside valuable cultural objects. The results of the neutron studies of several archaeological objects related to different epochs of the Russian history are reported in order to demonstrate the opportunities provided by the neutron tomography method. The obtained 3D structural volume data, as well as the results of the corresponding data analysis, are presented.

Keywords: neutron imaging; neutron; tomography; cultural heritage

1. Introduction

One of the most important tasks of archeology and other history-related sciences is the comprehensive study of cultural heritage items. The results of these studies have a significant application value, because they provide a way to penetrate into the far past and allow us to understand the formation and evolution of civilizations and ethnic groups. The experimental methods applied to characterize archeological and cultural heritage items are used to obtain detailed data regarding the phase analysis, assembly of inner parts and design items, the evolution of cracks and defects, and the traces of corrosion propagation [1]. Valuable and irreplaceable archaeological items are part of the cultural heritage of nations, requiring innovative approaches to their study in order to ensure their physical preservation for future generations. It is desirable to investigate them by modern non-destructive methods [2]. One of the non-destructive methods is X-ray tomography, which makes it possible to obtain three-dimensional (3D) visual data with a good precision for use both in qualitative and quantitative studies [3]. However, X-ray tomography methods, including those applied using synchrotron radiation sources, have some restrictions with respect to the dimensions of the objects under study, and the worsening of the imaging data due to X-ray attenuation by metals, resulting in beam hardening. Thus, there are limits on the sample sizes that can be examined. A complementary method to X-ray tomography is neutron radiography and tomography [3–6]. The fundamental difference in the nature of neutron interactions with matter compared to X-rays provides additional benefits to neutron methods, including sensitivity to light elements, a notable difference in contrast between different metals, and high penetration ability. All these features make neutron tomography an attractive tool, with a growing range of applications in industry, geophysics and paleontology [7,8].

The non-destructive character of the neutron radiography and tomography method has prompted the rising interest in studying rare archaeological items and museum rarities, especially metallic artifacts, weapons and ancient jewelry [9–11]. It should be emphasized that neutron radiography and tomography have been successfully used to analyze relatively large bronze objects of the Roman period [9], arms from medieval Europe and Japan [10], lead sculptures, and urns [11]. The obtained structural information allows one to understand the cultural origin of an object, determining a technological approach and strategies for future preservation or restoration of the cultural heritage items.

Recently, there has been a significant increase in successful cooperation between the Joint Institute for Nuclear Research and the Institute of Archeology of the Russian Academy of Sciences. The complementary archaeological and physical research makes it possible to study a large number of valuable objects from various large-scale archaeological excavations in the territory of the Russian Federation. Examples of the scientific achievements resulting from this cooperation, as well as a demonstration of the opportunities provided by neutron radiography and tomography methods, are given in this paper. We present several interesting results of neutron studies of the historical and cultural heritage objects dating to different periods of the nation's history. This is the result of neutron imaging studies of fragments of metal parts retrieved from the underwater remains [12] of the bireme of the king Mithridates VI Eupator. These items were found at the National Archaeological Museum "Phanagoria". Another object representing a different historical era is the golden vial of an ancient Sarmatian woman from the burial "Chebotarev-5" [13]. This paper also shows the results of the studies of ancient fibulae from the Viking age from Podbolotie burial excavations [14]. Here, the neutron tomography data help to interpret the specifics of the production technology of such fibulae, and relate this ancient jewelry with well-known finds in the Western and Northern Europe. This work presents the visual 3D structural volume data of the studied cultural heritage objects, as well as the results of the corresponding analysis.

2. Materials and Methods

The studied cultural heritage items were obtained from the storage collection of the Institute of Archeology of the Russian Academy of Sciences. A fragment of the metal parts (Figure 1a) of the underwater remains of bireme [12] of the king Mithridates VI Eupator was found at the National Archaeological Museum "Phanagoria", located on the shore of Taman city. This archeological item is originated during the period of suppression of the insurrection in the ancient Greek polis Phanagoria, in the first century BC. The studied fragment of the bireme remains is covered with a blue-green corrosion layer mixed with silt bottom deposits. This type of corrosion on copper items causes the formation of cuprite Cu_2O fractions on the surface, with the subsequent gradual destruction of the initial metallic sample. The golden vial (Figure 1b) was extracted from the rich burial site of a Sarmatian woman at the "Chebotarev-5" archeological site [13] close to Rostov-on the-Don city. The well-preserved handles of the vial and the decoration on the top are visible. However, the internal volume of the closed vial remains hidden. A photo of the ancient fibulae is shown in Figure 1c. The golden ornament on the copper body of the fibulae is clearly visible, but the internal structure of the fibulae and the places of the previous restoration have been studied less.

The neutron tomography experiments were performed at the neutron radiography and tomography facility [15,16] located on beamline 14 of the IBR-2 reactor. The IBR-2 reactor is one of the most powerful pulsed neutron sources in the world, with the average power of 2 MW, a power per neutron pulse of 1850 MW, and a neutron flux in pulse of $5 \; 10^{15}$ n/cm^2/s [17]. The pulsed operation regime of the IBR-2 reactor is at a frequency of 5 Hz, and the long pulse duration for thermal neutrons of 350 μs makes it attractive not only for traditional neutron imaging applications, but also for the development of modern energy-selective techniques used in time-of-flight methods [18]. The IBR-2 reactor provides a thermal neutron beam with wavelengths ranging from ~0.2 to 8 Å and a spectral distribution maximum of ~1.8 Å. The neutron flux at the sample position is $\Phi = 5.5(2) \times 10^6$ n/cm^2/s.

A set of neutron radiography images was collected by a CCD-based detector system with a maximum field of view of 20 cm × 20 cm. A dedicated detector module with two mirrors to suppress parasitic neutron scattering was used (Figure 2). The neutron beam dimensions restricted the upper limit of the sample size to 20 cm. The tomography experiments were performed with a rotation step of 0.5°, and the total number of measured radiography projections was 360. The obtained imaging data were corrected by subtracting the camera dark current image, and were normalized to the image of the incident neutron beam using the ImageJ software [19]. The exposure time for one projection was 10 s, and the resulting measurements lasted for 4 h for each sample.

(**a**) (**b**) (**c**)

Figure 1. Photos of the studied cultural heritage objects: (**a**) the fragment of remains of ancient bireme; (**b**) golden vial of a Sarmatian woman; and (**c**) fibulae.
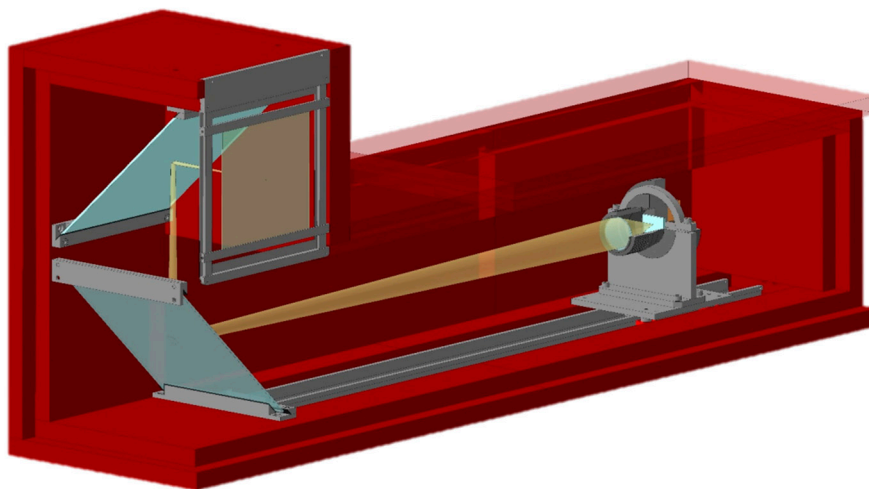

Figure 2. Scheme of the detector system used on the neutron radiography and tomography facility on the IBR-2 reactor. Firstly, the neutron radiation is converted into light photons by a scintillator plate. The scintillator thickness is 100 µm. The light from the scintillator is reflected by the mirrors, and then directed to the optical system of the high resolution and high sensitive CCD-based video camera.

It should be noted that radioactive activation of the studied samples during the neutron tomography experiments is an urgent problem. One way of suppressing this negative effect is to reduce the exposure time by decreasing the number of corresponding angular projections. The iterative reconstruction algorithms for tomography have demonstrated promising results in the ability to compute high-quality 3D images from less data. In which case, the application of iterative algorithms like the Simultaneous Iterative Reconstruction Technique (SIRT) [20], the Simultaneous Algebraic Reconstruction Technique (SART) [21], or other more complex techniques [22] for tomography

reconstruction calculations allows qualitative data to be obtained. The ASTRA Toolbox [23] is a MATLAB and Python platform providing high-performance GPU primitives for 2D and 3D tomography, including building blocks for advanced reconstruction algorithms. One of its main design goals is geometric flexibility, allowing the toolbox to be used with many types of experimental setups.

For a brief demonstration of the possibilities of iterative reconstruction algorithms, in Figure 3 we present the comparative images of tomography slices reconstructed by means of different reconstruction algorithms. We ran 150 iterations for the iterative algorithms for neutron imaging data of the studied gold vial. The tested neutron data consisted of 380 projections with dimensions of 1311×1392. It seems that the use of iterative algorithms could reduce the number of projections required for tomography reconstruction; however, it would require longer times for reconstruction of large volumes. The reduction of calculation time is possible by using specialized professional graphics cards with CUDA technology [24] support. However, in order to use the ASTRA toolbox, the user requires the skills necessary to parse and process data in the MATLAB or Python layer [23,25]. Moreover, the algorithms bundled in the ASTRA Toolbox are limited to reconstruction methods, and do not include typical image pre-processing, like flat field correction or rotation center calculation algorithms. These disadvantages limit the target audience of the ASTRA Toolbox mainly to researchers and users with an expertise in computer science. In the framework of our research of cultural heritage objects, and in the case of a full set of neutron tomography projections, the use of the conventional Filtered Backprojection (FBP) algorithm [26] seems reasonable and sufficient for our study aims.

(a)   (b)   (c)
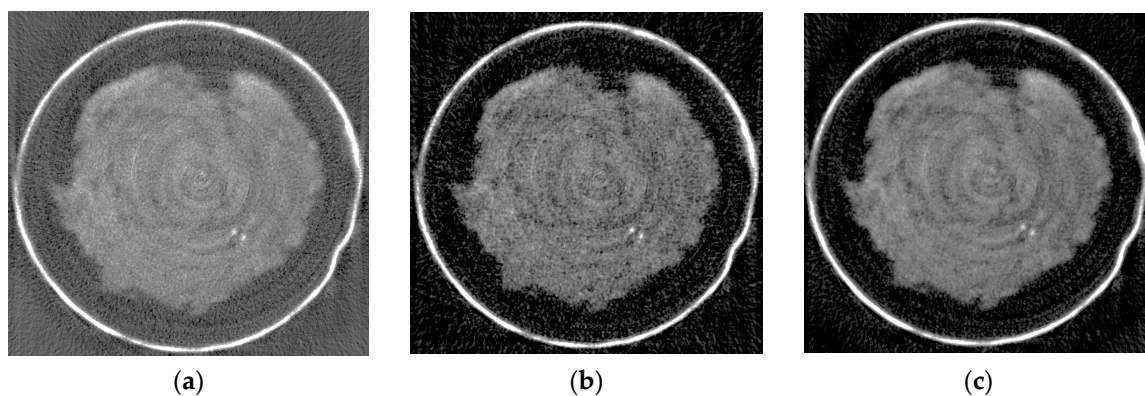
Figure 3. The examples of the tomography slices of the golden vial reconstructed by the conventional FBP algorithm (**a**), by the SIRT reconstruction with 150 iterations (**b**), by the SART algorithm with 150 iterations (**c**).

The H-PITRE software [27] was used for the tomography reconstruction . An algorithm [28] for reducing ring-shaped artifacts was applied. The size of one voxel in our study is 42 μm × 42 μm × 42 μm. Each of the voxels is characterized by spatial coordinates in the reconstructed 3D volume, and a specific value of a shade of grey color. The 3D volume data of voxels are the essence of the spatial distribution of values of the neutron attenuation coefficients inside the sample volume. Attenuation of the neutron beam corresponds to scattering and absorption losses inside the material. It is accepted [4] that neutron attenuation processes are described by total scattering cross-sections as the sum of neutron scattering and absorption cross-sections, or by the attenuation length. The spatial resolution capabilities of the neutron tomography facility impose some restrictions on the minimum size of a resolved item, up to 270 microns or 0.02 mm^3.

The VGStudio MAX 2.2 software of Volume Graphics (Heidelberg, Germany) was used for visualization and analysis of the reconstructed 3D data. The FEI Aviso 3D software was applied for the skeletonization procedure. In addition, specialized plug-ins for the ImageJ software, like Segmentation3D [29], Local Thickness [30] and Skeletonize3D [31] were used for quantitative analysis of the obtained 3D volume data.

3. Results and Discussion

### 3.1. Neutron Tomography Studies of the Fragment of the Bireme Remains

A typical example of neutron radiographic images used in the tomography process to reconstruct the internal structure of the remains fragment is shown in Figure 4a. The inner part, containing copper, contrasts well with the covered corrosion layer in the neutron radiography experiments. The attenuation of the neutron beam corresponds to the scattering and absorption losses inside the matter. The neutron attenuation processes are described by total scattering cross-sections as a sum of neutron scattering and absorption cross-sections, or by the attenuation length [4]. The neutron attenuation coefficients for a neutron beam of copper are larger in comparison to the relevant parameters for silt deposits. Due to this fact, it is quite easy to recover the hidden object in the corrosion shell. The 3D models of the bireme fragment reconstructed from the neutron tomography data are presented in Figure 4b. Inside the fragment volume, a well-shaped fragment of a nail or a pin is clearly visible. The total 3D reconstructed volume of the fragment of the bireme was virtually divided into two separated volumes, corresponding to the corrosion layer volume and the volume of the copper remains. The separated 3D volume of the metal inclusion in the studied fragment volume is shown in Figure 4c. In accordance with the presented 3D model, the copper remains retain the shape of an ancient nail. The volumetric calculations to obtain dimensions and volumes of the nail were performed. The average volume of the observed copper remains is 1739.47(3) mm^3. The mean height of the nail is 67.4 mm, the estimated diameter of the nail head is ~8 mm.

(**a**)   (**b**)   (**c**)
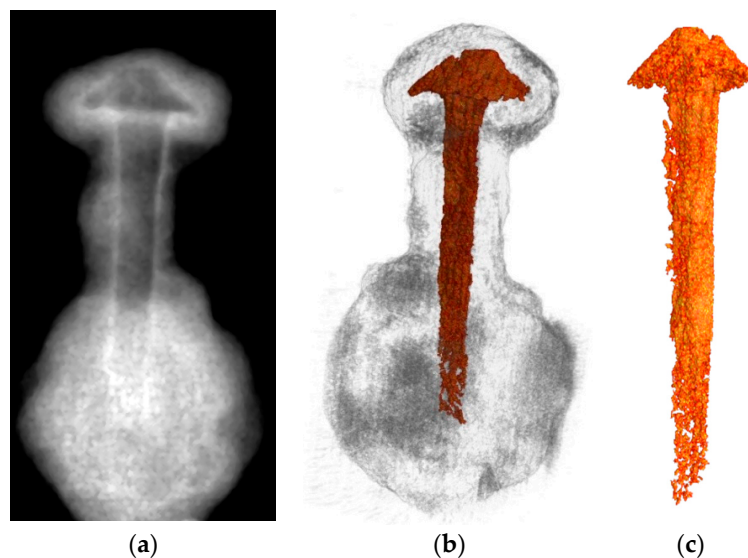
Figure 4. (**a**) The neutron radiography image of the fragment of the bireme remains; the background is black; (**b**) the virtual 3D model of the fragment of the bireme remains, the copper remains are labeled in a dark yellow color, the corrosion component is grey; the corrosion components are made more transparent for clarity; (**c**) the separated 3D volume of the metal inclusion in the bireme fragment.

3.2. The Neutron Studies of the Golden Vial

After the tomography reconstruction procedure, we obtained a large set of images corresponding to different transverse slices of the studied vial. Examples of the neutron radiographic images, as well as the tomography slices of the golden vial, are shown in Figure 5a,b. The grey regions correspond to the fossils of internal fills; the light areas are the gold walls of the vial. The virtual slice of the reconstructed 3D model of the vial is presented in Figure 5b. The fossilized remnants of the supposed incense are a formless piece with a volume of 3162 mm^3. The total volume of the golden material is 615 mm^3.
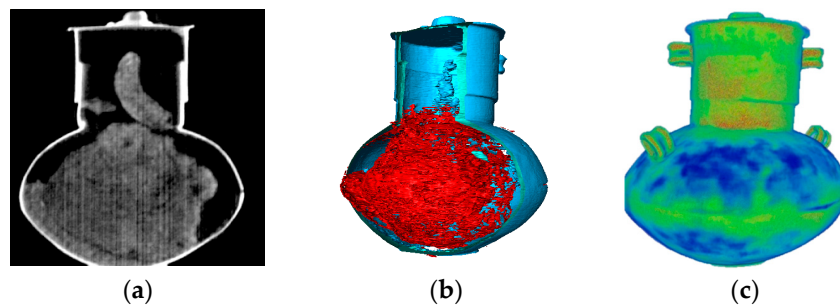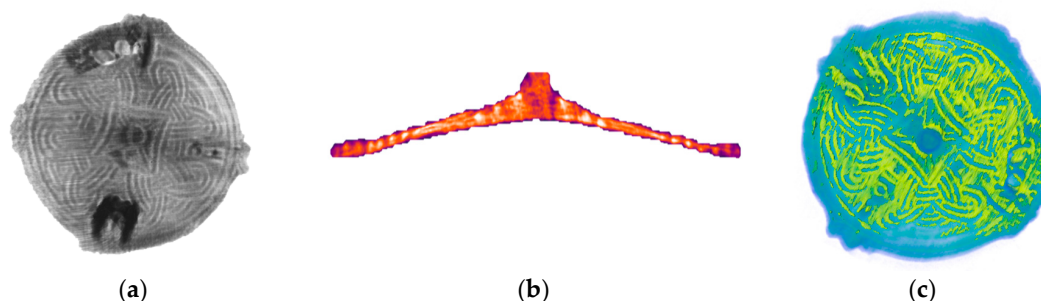
Figure 5. (**a**) The neutron radiography image of the golden vial. The bright regions correspond to high neutron attenuation in the gold component. The dark areas are the low neutron attenuation regions of the fossilized incense. The background is black. (**b**) Virtual slices of the 3D model of the studied golden vial. (**c**) The 3D model of the golden vial obtained after calculations by the Local Thickness method. A color scheme whereby the density of the neutron attenuation degree extends from low (blue) to high (red) is used.

We applied a dedicated Local Thickness algorithm [30] for the 3D data treatment. The result of these calculations is a spatial distribution of the density of the neutron attenuation coefficients, corrected for the complex 3D shape of the golden vial. In other words, we obtained a spatial distribution of the thickness deviation of the golden wall. The obtained 3D model is presented in Figure 5d. It can be seen that the deviations in the thickness of the vessel wall are minimal, which indicates the fine work and high skills of the ancient master [13]. The joint track between the two hemispherical parts of the main body of the vial is clearly visible.

3.3. The Neutron Tomography Study of the Fibulae

A typical example of the neutron radiographic images used in the tomography reconstruction process of the fibulae is shown in Figure 6a. The fragments of fasteners and clasps of the fibulae can be clearly seen. The neutron absorption coefficients for neutrons of the gold are significantly larger in comparison to the relevant parameters for copper. Therefore, the golden ornament contrasts well with the copper body in the neutron radiography experiments (Figure 6a). The virtual cut of the 3D model of the fibulae is presented in Figure 6b. The virtual cut of the 3D model of the fibulae shows the golden thread, which is deeply pressed into the thickness of the copper body of the fibulae. This fact directly indicates the use of old Scandinavian production technology [32]. It can be assumed that the ancient burial place in Podbolotie was the burial place of a rich Viking warrior [33].

Figure 6. (**a**) The neutron radiography image of the fibulae. The bright regions correspond to high neutron attenuation in the golden component; the darker areas are the low neutron attenuation regions of copper. The parts of the remains of clasp on the reverse size of the fibulae are dark; (**b**) the axial tomography slice of the fibulae are presented as an example; the light areas correspond to gold inclusions, the orange regions are the copper body; (**c**) the virtual 3D model of the fibulae with separated golden ornament.

The main difficulty was the correct segmentation of the copper base and the golden ornament. The thickness of the gold threads of the golden ornament were near the resolution limit of our neutron radiography facility. Furthermore, there is the destruction of the golden pattern due to the corrosion processes. We employed various methods of image separation, and the total 3D reconstructed volume of the fibulae was divided into two separate volumes, corresponding to the copper base and the golden components. We employed various methods of image separation, and then virtually divided the gold and copper components of the fibulae (Figure 6c). The statistical analysis provides the average thickness of the gold layers. The mean thickness of the gold in the ornament is 0.73(1) mm, the median value is 0.54(2) mm.

4. Conclusions

The obtained neutron tomography results demonstrate the opportunities offered by the neutron tomography method for non-destructive testing of large metallic cultural heritage artefacts. A 3D analysis of the interior of the studied items was performed. Morphological calculations based on the experimental tomography data were used to analyze the spatial arrangement of different components of the studied objects. The neutron imaging contrast in the neutron attenuation coefficients between different components allowed us to clarify several specifics related to the ancient production technologies of the above cultural heritage objects. The obtained characteristics of the internal structures of the studied objects are important for further development of existing archeological and historical concepts.

Author Contributions: Irina Saprykina, Denis Kozlenko and Sergey Kichanov conceived and designed the neutron experiments; Irina Saprykina contributed materials for investigation and described the archeological and historical related background in the manuscript; Kuanysh Nazarov and Anton Rutkauskas performed the neutron radiography experiments; Kuanysh Nazarov and Evgenii Lukin made a preliminary imaging data treatments; Sergey Kichanov and Boris Savenko performed tomography reconstruction and analyzed the 3D data; Sergey Kichanov and Denis Kozlenko prepared the main manuscript text and display items. All authors reviewed the manuscript.

References

1. Middleton, A.; Tum, J. *Radiography of Cultural Material*, 2nd ed.; Lang, J., Ed.; Taylor & Francis Ltd.: Oxford, UK, 2005; p. 208, ISBN 0750663472.
2. *Non-Destructive Micro Analysis of Cultural Heritage Materials*, 1st ed.; Janssens, K., Van Grieken, R., Eds.; Elsevier Science: Amsterdam, The Netherlands, 2004; p. 828, ISBN 0444507388.
3. Mannes, D.; Schmid, F.; Frey, J.; Schmidt-Ott, K.; Lehmann, E. Combined neutron and X-ray imaging for non-invasive investigations of cultural heritage objects. *Phys. Procedia* **2015**, *69*, 653–660. [CrossRef]
4. *Neutron Imaging and Applications: A Reference for the Imaging Community*; Anderson, I.S., McGreevy, R.L., Bilheux, H.Z., Eds.; Springer: New York, NY, USA, 2009; p. 341.
5. Lehmann, E.; Kaestner, A.; Gruenzweig, C.; Mannes, D.; Vontobel, P.; Peetermans, S. Materials research and non-destructive testing using neutron tomography methods. *Int. J. Mater. Res.* **2014**, *105*, 664–670. [CrossRef]
6. Peetermans, S.; Lehmann, E. Simultaneous neutron transmission and diffraction contrast tomography as a non-destructive 3D method for bulk single crystal quality investigations. *J. Appl. Phys.* **2013**, *114*, 124905. [CrossRef]
7. Peetermans, S.; Grazzi, F.; Salvemini, F.; Lehmann, E.; Caporali, S.; Pratesi, G. Energy-selective neutron imaging for morphological and phase analysis of iron-nickel meteorites. *Analyst* **2013**, *138*, 5303–5308. [CrossRef] [PubMed]
8. Perfect, E.; Cheng, C.L.; Kang, M.; Bilheux, H.Z.; Lamanna, J.M.; Gragg, M.J.; Wright, D.M. Neutron imaging of hydrogen-rich fluids in geomaterials and engineered porous media: A review. *Earth-Sci. Rev.* **2014**, *129*, 120–135. [CrossRef]
9. Lehmann, E.; Deschler-Erb, E.; Ford, A. Neutron Tomography as a valuable tool for the non-destructive analysis of historical bronze scultures. *Archaeometry* **2010**, *52*, 272. [CrossRef]

10. Salvemini, F.; Grazzi, F.; Fedrigo, A.; Williams, A.; Civita, F.; Scherillo, A.; Vontobel, P. Hartmann, S.; Lehmann, E.; Zoppi, M. Revealing the secrets of composite helmets of ancient Japanese tradition. *Eur. Phys. J. Plus* **2013**, *128*, 87. [CrossRef]

11. Harvig, L.; Lynnerup, N.; Ebsen, J. Computed tomography and computed radiography of late Bronze Age cremation urns from Denmark: An interdisciplinary attempt to develop methods applied in bioarcheological cremation research. *Archaeometry* **2012**, *54*, 369–387.

12. Zhukovsky, M.O.; Kuznetsov, V.D.; Olkhovsky, S.V. Photogrammetric techniques for3-D underwater record of the antique time ship from Phanagoria. *Int. Arch. Photogramm. Remote Sens. Spat. Inf. Sci.* **2013**, *40*, 717–721. [CrossRef]

13. Rychkov, S.; Morozova, I.; Grocheva, A.; Kovalevskaia, V. Genetic Structure of Sarmatians from Cis-Asov Steppe (1 century B.C.). In Proceedings of the 18th Congress of the European Anthropological Association, Ankara, Turkey, 3–6 September 2012; Human Evolution and Dispersals: Ankara, Turkey, 2012; p. 14.

14. Saprykina, I.A.; Zelentsova, O.V. The results of using natural science methods in identifying the criteria for determining status burials on the basis of integrated analysis of 8th–11th cc. belt sets from Mordovian graves. In Proceedings of the Lasmac-2011, Cancun, Mexico, 23–27 January 2011; p. 246.

15. Kozlenko, D.P.; Kichanov, S.E.; Lukin, E.V.; Rutkauskas, A.V.; Bokuchava, G.D.; Savenko, B.N.; Pakhnevich, A.V.; Rozanov, A.Y. Neutron Radiography Facility at IBR-2 High Flux Pulsed Reactor: First Results. *Phys. Procedia* **2015**, *69*, 87–91. [CrossRef]

16. Kozlenko, D.P.; Kichanov, S.E.; Lukin, E.V.; Rutkauskas, A.V.; Belushkin, A.V.; Bokuchava, G.D.; Savenko, B.N. Neutron radiography and tomography facility at IBR-2 reactor. *Phys. Part. Nucl. Lett.* **2016**, *13*, 346–351. [CrossRef]

17. Pepelyshev, Y.N.; Popov, A.K.; Sumkhuu, D. IBR-2M Reactor Power Feedback Parameters Evaluation Using Square Reactivity Oscillations. *At. Energy* **2017**, *122*, 75–80. [CrossRef]

18. Kockelmann, W.; Frei, G.; Lehmann, E.H.; Vontobel, P.; Santisteban, J.R. Energy-selective neutron transmission imaging at a pulsed source. *Nucl. Instrum. Methods Phys. Res. A* **2007**, *578*, 421–434. [CrossRef]

19. Schneider, C.A.; Rasband, W.S.; Eliceiri, K.W. NIH Image to ImageJ: 25 years of image analysis. *Nat. Methods* **2012**, *9*, 671–675. [CrossRef] [PubMed]

20. Gregor, J.; Benson, T. Computational analysis and improvement of SIRT. *IEEE Trans. Med. Imaging* **2008**, *27*, 918–924. [CrossRef] [PubMed]

21. Andersen, A.H.; Kak, A.C. Simultaneous algebraic reconstruction technique (SART): A superior implementation of the art algorithm. *Ultrason. Imaging* **1984**, *6*, 81–94. [CrossRef] [PubMed]

22. Chang, J.-H.; Anderson, J.M.M.; Votaw, J.T. Regularized image reconstruction algorithms for positron emission tomography. *IEEE Trans. Med. Imaging* **2004**, *23*, 1165–1175. [CrossRef] [PubMed]

23. Van Aarle, W.; Palenstijn, W.J.; Cant, J.; Janssens, E.; Bleichrodt, F.; Dabravolski, A.; De Beenhouwer, J.; Batenburg, K.J.; Sijbers, J. Fast and Flexible X-ray Tomography Using the ASTRA Toolbox. *Opt. Express* **2016**, *24*, 25129–25147. [CrossRef] [PubMed]

24. Pang, W.M.; Qin, J.; Lu, Y.; Xie, Y.; Chui, C.K.; Heng, P.A. Accelerating simultaneous algebraic reconstruction technique with motion compensation using CUDA-enabled GPU. *Int. J. Comput. Assist. Radiol. Surg.* **2011**, *6*, 187–199. [CrossRef] [PubMed]

25. Palenstijn, W.J.; Bédorf, J.; Sijbers, J.; Batenburg, K.J. A distributed ASTRA toolbox. *Adv. Struct. Chem. Imaging* **2017**, *2*, 2–15. [CrossRef] [PubMed]

26. Herman, G.T. *Fundamentals of Computerized Tomography: Image Reconstruction from Projection*, 2nd ed.; Springer Science & Business Media: Berlin, Germany, 2009; p. 300, ISBN 978-1-84628-723-7.

27. Chen, R.C.; Dreossi, D.; Mancini, L.; Menk, R.; Rigon, L.; Xiao, T.Q.; Longo, R. PITRE: Software for phase-sensitive X-ray image processing and tomography reconstruction. *J. Synchrotron Radiat.* **2012**, *19*, 836–845. [CrossRef] [PubMed]

28. Münch, B.; Trtik, P.; Marone, F.; Stampanoni, M. Stripe and ring artefact removal with combined wavelet—Fourier filtering. *Opt. Express* **2009**, *17*, 8567–8591. [CrossRef] [PubMed]

29. Ollion, J.; Cochennec, J.; Loll, F.; Escudé, C.; Boudier, T. TANGO: A generic tool for high-throughput 3D image analysis for studying nuclear organization. *Bioinformatics* **2013**, *29*, 1840–1841. [CrossRef] [PubMed]

30. Dougherty, R.P.; Kunzelmann, K.-H. Computing Local Thickness of 3D Structures with ImageJ. *Microsc. Microanal.* **2007**, *13*, 1678–1679. [CrossRef]

31.　Sato, M.; Bitter, I.; Bender, M.A.; Kaufman, A.E.; Nakajiama, M. TEASAR: Tree-structure extraction algorithm for accurate and robust skeletons. In Proceedings of the Eighth Pacific Conference on Computer Graphics and Applications, Hong Kong, China, 5 October 2000; pp. 271–449.

32.　Gavritukhin, I. For the Study of the Nature of Relations between the South of the East Europe and the Central Region of the North Europe in the Late Period of Roman Influence and Great Migration Period. In *Inter Ambo Maria. Contacts between Scandinavia and Crimea in the Poman Period*; Dolya Publishing House: Simferopol, Crimean Peninsula, 2010; pp. 28–33.

33.　Terekhova, N.N.; Zavyalov, V.I. The Scandinavian traditions in the blacksmith craft of Northern Rus. In Proceedings of the 3rd International conference Archaeometallurgy in Europe, Bochum, Germany, 29 June–1 July 2011.